

10
12-10-96 Q8 (1)

LBNL-39450
UC-413



ERNEST ORLANDO LAWRENCE BERKELEY NATIONAL LABORATORY

Radiation Shielding and Patient Organ Dose Study for an Accelerator-Based BNCT Facility at LBNL

S.V. Costes, R.J. Donahue, and J. Vujic
**Environment, Health
and Safety Division**

October 1996



DISCLAIMER

This document was prepared as an account of work sponsored by the United States Government. While this document is believed to contain correct information, neither the United States Government nor any agency thereof, nor The Regents of the University of California, nor any of their employees, makes any warranty, express or implied, or assumes any legal responsibility for the accuracy, completeness, or usefulness of any information, apparatus, product, or process disclosed, or represents that its use would not infringe privately owned rights. Reference herein to any specific commercial product, process, or service by its trade name, trademark, manufacturer, or otherwise, does not necessarily constitute or imply its endorsement, recommendation, or favoring by the United States Government or any agency thereof, or The Regents of the University of California. The views and opinions of authors expressed herein do not necessarily state or reflect those of the United States Government or any agency thereof, or The Regents of the University of California.

Available to DOE and DOE Contractors
from the Office of Scientific and Technical Information
P.O. Box 62, Oak Ridge, TN 37831
Prices available from (615) 576-8401

Available to the public from the
National Technical Information Service
U.S. Department of Commerce
5285 Port Royal Road, Springfield, VA 22161

Ernest Orlando Lawrence Berkeley National Laboratory
is an equal opportunity employer.

DISCLAIMER

**Portions of this document may be illegible
in electronic image products. Images are
produced from the best available original
document.**

Radiation Shielding and Patient Organ Dose Study for an Accelerator-Based BNCT Facility at LBNL

S. V. Costes^a, R. J. Donahue^b and J. Vujic^a

^a Nuclear Engineering Department, University of California, Berkeley, CA 94720

^b Lawrence Berkeley National Laboratory, Berkeley, CA 94720

ABSTRACT

This study considers the radiation safety aspects of several designs discussed in a previous report¹ of an accelerator-based source of neutrons, based on the ${}^7\text{Li}(p,n)$ reaction, for a Boron Neutron Capture Therapy (BNCT) Facility at LBNL. The first part of this paper determines the optimal radiation shield thicknesses for the patient treatment room. Since this is an experimental facility no moderator or reflector is considered in the bulk wall shield design. This will allow the flexibility of using any postulated moderator/reflector design and assumes sufficient shielding even in the absence of a moderator/reflector. In addition the accelerator is assumed to be capable of producing 100 mA of 2.5 MeV proton beam current. The addition, of 1% and 2% ${}^{10}\text{B}$ (by weight) to the concrete is also investigated.

The second part of this paper determines the radiation dose to the major organs of a patient during a treatment. Simulations use the MIRD 5 anthropomorphic phantom² to calculate organ doses from a 20 mA proton beam assuming various envisioned moderator/reflector in place. Doses are tabulated by component and for a given uniform ${}^{10}\text{B}$ loading in all organs. These are presented in Table 8 for a BeO moderator and in Table 7 for an Al/AlF₃ moderator. Dose estimates for different ${}^{10}\text{B}$ loadings may be scaled.

This work was supported by the Director, Office of Energy Research, Nuclear Physics Division of the Office of High Energy and Nuclear Physics, of the U. S. Department of Energy under Contract DE-AC03-76SF00098

DISTRIBUTION OF THIS DOCUMENT IS UNLIMITED



MASTER

Shielding of Treatment Room

Radiation shield walls will be necessary to reduce neutron and photon dose rates outside the patient treatment room to personnel working nearby. In this section we determine the necessary concrete shield thickness. All analyses are performed with the MCNP³ Monte Carlo radiation transport code.

Table 1: Fluence-to-Dose Equivalent Conversion Factors used in shielding analysis.

Neutron Energy (MeV)	Conversion Factor (cSv/cm ²)	Neutron Energy (MeV)	Conversion Factor (cSv/cm ²)
1.0000E-11	9.0949E-10	7.4274E-01	2.6936E-08
4.1400E-07	8.5766E-10	9.0718E-01	2.8535E-08
1.1254E-06	8.5000E-10	1.1080E+00	3.0488E-08
2.3824E-06	8.5000E-10	1.3534E+00	3.2042E-08
5.0435E-06	8.4603E-10	1.6530E+00	3.3787E-08
1.0677E-05	8.4698E-10	2.0190E+00	3.5338E-08
2.2603E-05	9.1331E-10	2.4660E+00	3.6701E-08
1.0130E-04	1.0325E-09	3.0119E+00	3.8101E-08
4.5400E-04	1.0800E-09	3.6788E+00	3.8977E-08
1.5846E-03	1.0653E-09	4.4933E+00	4.0047E-08
3.3546E-03	1.2009E-09	5.4881E+00	4.0496E-08
7.1018E-03	1.6351E-09	6.7032E+00	4.1000E-08
1.5034E-02	2.6368E-09	8.1873E+00	4.1152E-08
3.1828E-02	5.0702E-09	1.0000E+01	4.1066E-08
8.6517E-02	9.1843E-09	1.2214E+01	4.1140E-08
1.4996E-01	1.2615E-08	1.3499E+01	4.1924E-08
2.2371E-01	1.6178E-08	1.4918E+01	4.3067E-08
3.3373E-01	2.0227E-08	1.7500E+01	4.4440E-08
4.9787E-01	2.4162E-08		

Flux-to-dose equivalent conversion factors are taken from Belogorlov⁴. These conversion factors were calculated by Belogorlov by considering the energy deposition in an semi-infinite slab of tissue from monoenergetic neutron beams as a function of depth. These are shown in Table 1.

The assumed layout of the patient treatment room is shown in Fig. 1. All walls are assumed to be 480 cm from the target to the inside of the shield wall. All walls

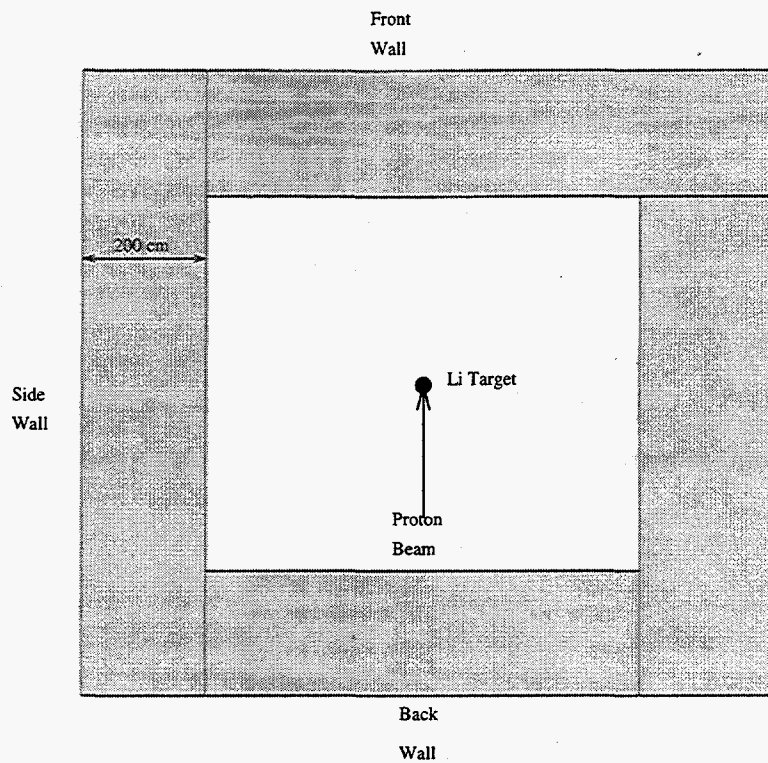


Figure 1: Layout of a patient treatment room with concrete shield walls.

initially are 200 cm thick with a density of 2.35 g/cm^3 . Concrete composition⁵ used is shown in Table 2.

Table 2: Elemental concrete composition used in these analyses.

Concrete Composition	
Element	Partial Density (g/cm^3)
H	0.013
O	1.165
Si	0.737
Ca	0.194
Na	0.040
Mg	0.006
Al	0.107
S	0.003
K	0.045
Fe	0.029

The neutron spectrum from the ${}^7\text{Li}(p,n)$ reaction is taken from a previous report¹ for an incident 2.5 MeV proton beam of 100 mA. The current accelerator design is based on delivering at least 20 mA but possibly as high as 100 mA. Therefore the radiation shielding is based on a beam current of 100 mA. No moderator or reflector is assumed to be present, *i.e.*, the target is bare. This is to ensure that the shield design is independent of a particular moderator/reflector configuration. This will allow for the flexibility of experimenting with various moderator/reflector designs and for neutron spectra measurements without the moderator/reflector.

Biological dose equivalents are computed by converting the neutron and gamma fluxes to dose equivalent at different depths in a single thick shield wall *i.e.*, one simulation is done and dose equivalent rates are examined at various depths as opposed to the more correct approach of doing separate simulations for each thickness and tallying the dose equivalent rate immediately outside the shield wall. The effect of this is to increase the dose equivalent by including the contributions due to backscatter within the shield wall. This greatly reduces the number of simulations to be made and is estimated to increase the dose equivalent by no more than a factor of two. This is acceptable for radiation protection purposes and errs on the side on conservatism.

All neutron and photon scoring is done using the MCNP point detector tally. This is a biased tally whereby an estimate is made to the tally location of all interactions in the shield, whether or not the particle ever reaches the actual detector location. This is a very efficient technique for such deep penetration problems and results in good statistical accuracy.

The results for the front wall (with respect to the proton beam) are shown in Fig. 2. From this it can be seen that the gamma dose exceeds the neutron dose for thicknesses greater than about 60 cm due to gamma production via (n,γ) thermal neutron capture. Several trace elements in concrete have large thermal capture cross sections. In particular, ${}^{23}\text{Na}$ has a thermal capture cross section of about 500 mb. These capture gammas have a complex energy spectrum with energies from less than 1 MeV up to approximately 10 MeV.

Forward Wall

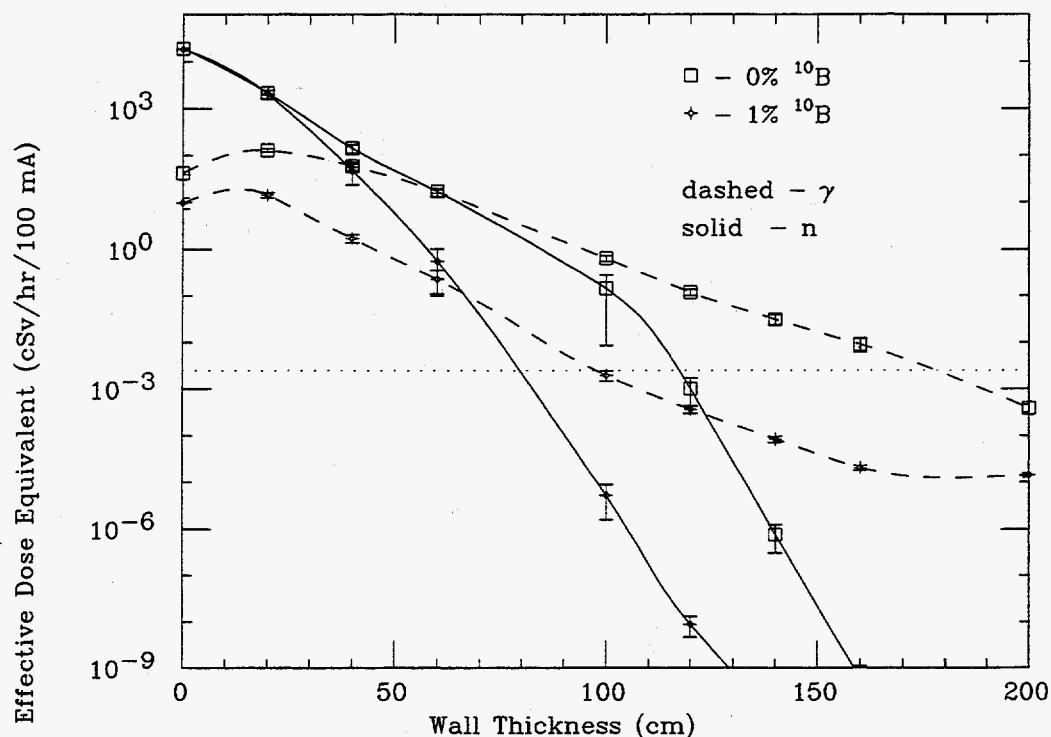


Figure 2: Dose equivalent rate as a function of concrete shield thickness for the front wall. The dotted line represents an acceptable occupational level.

To minimize the production of capture gammas we investigated the addition of ^{10}B to concrete. As is well known in BNCT, ^{10}B has a thermal absorption cross section of about 3800 b via the reaction $^{10}\text{B}(n,\alpha)$. The dose rate as a function of concrete thickness is shown in Fig. 2 for two cases: no ^{10}B and 1% ^{10}B by weight. As expected, the presence of ^{10}B produces a large drop in the depth dose curves. At a thickness of 50 cm the total dose equivalent rate has dropped by over two orders of magnitude relative to the results of unboronated concrete. Also of interest is that fact that the addition of 1% ^{10}B has the same net effect as the addition of 2% ^{10}B . It is therefore unnecessary to load the concrete with more than 1% by weight with ^{10}B .

After about 1 m of concrete the rate of attenuation reaches an asymptotic limit which is controlled by the gamma dose component. Fitting this data between 1 and 2 m gives a slope of about -0.08 cm^{-1} , or a mean free path of 12.5 cm.

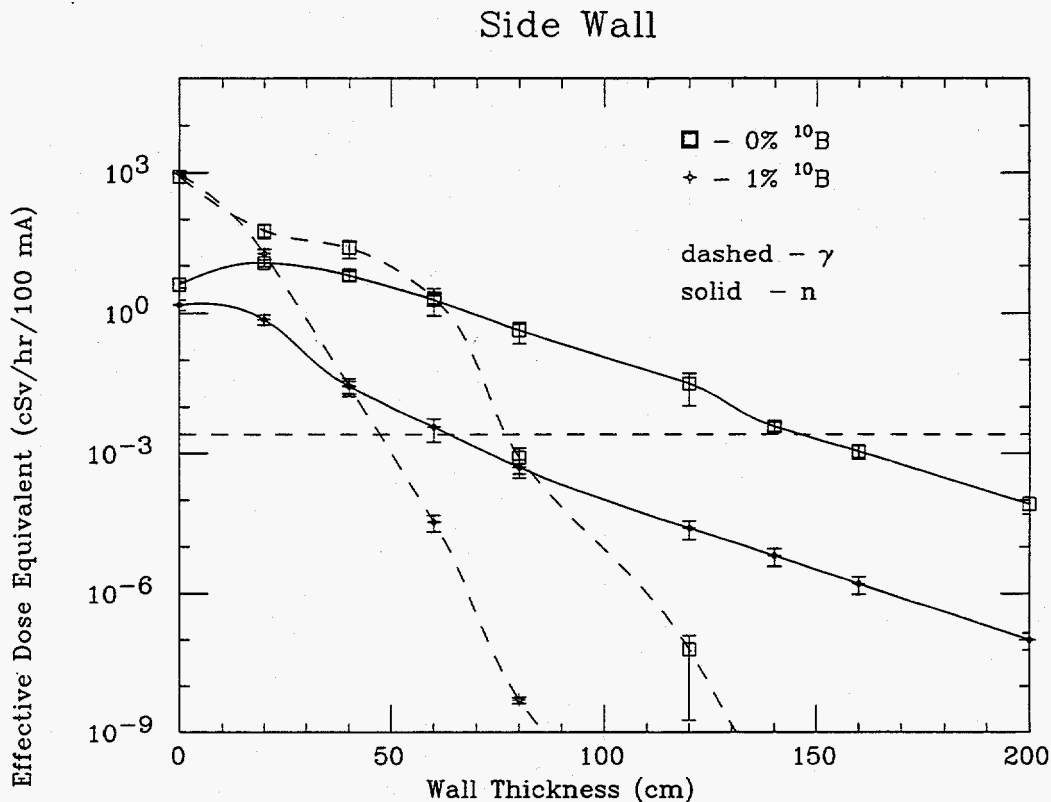


Figure 3: Dose rate as a function of concrete shield thickness for the side wall. The dotted line represents an acceptable occupational level.

Photon total cross sections have a minimum value in the region dominated by Compton scattering, referred to as the Compton minimum. The cross section for concrete at the Compton minimum ($E_\gamma = 4 \text{ MeV}$) is $0.0319 \text{ cm}^2/\text{g}$ which is equivalent to a mean free path of 13.34 cm. This agrees well with the mean free path determined above. Therefore, the dose at larger thicknesses may simply be extrapolated exponentially with a $1/e$ thickness (the thickness in which the dose has decreased by a factor of $1/e$) of about 13 cm. This corresponds to a factor of 10 reduction in the dose for every 30 cm additional concrete.

Similar dose equivalent rate versus concrete thickness plots for the side and back walls are shown in Fig. 3 and Fig. 4. On all depth dose plots a horizontal line at $2.5 \mu\text{Sv/hr}$ (2.5 mrem/hr) is shown. This corresponds to the DOE criteria of 5 cSv/yr (5 rem/yr) and a very conservative annual operation of 2000 hrs. A dose rate of $2.5 \mu\text{Sv/hr}$ also ensures that the area immediately outside the shield

Back Wall

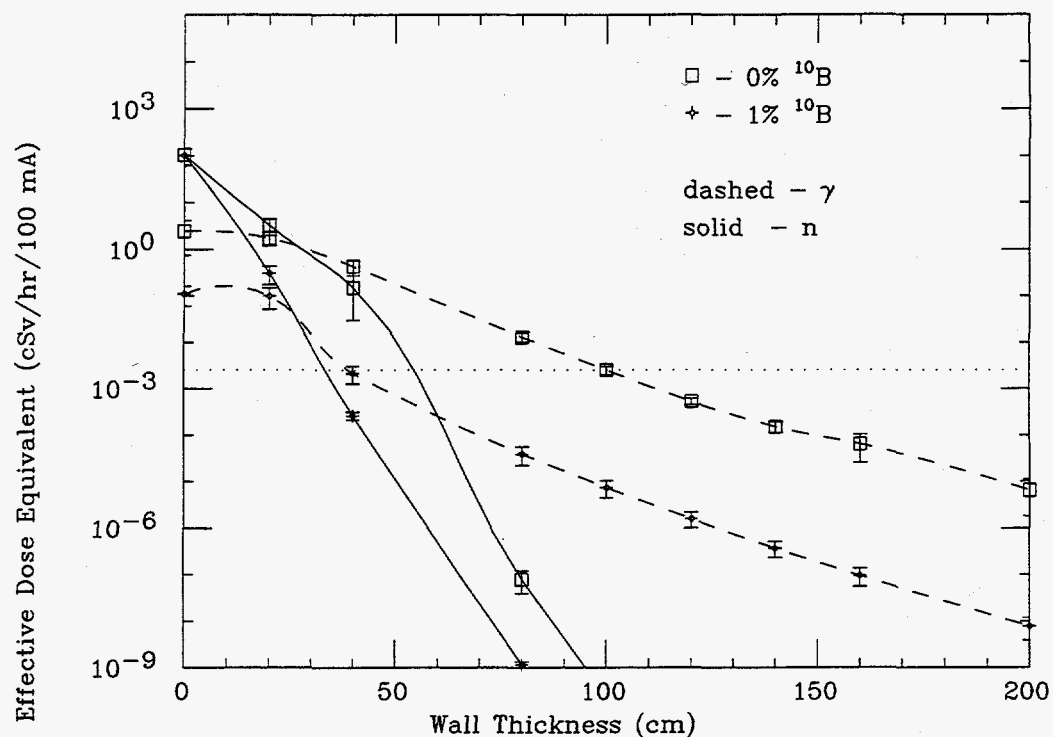


Figure 4: Dose equivalent rate as a function of concrete shield thickness for the back wall. The dotted line represents an acceptable occupational level.

Table 3: Concrete thicknesses to achieve $2.5 \mu\text{Sv/hr}$ (2.5 mrem/hr) from 100 mA, 2.5 MeV proton beam on ^7Li target.

	Concrete Thickness	
	No ^{10}B	1% ^{10}B
Forward Wall	180 cm	100 cm
Side Wall	145 cm	65 cm
Back Wall	100 cm	40 cm

% by weight

wall is below the threshold for becoming a DOE Radiation Area ($5 \mu\text{Sv/hr}$) which entails controlling ingress/egress, training, badging, etc. Table 3 summarizes the recommended shield thicknesses to achieve the above criteria for the case of normal concrete and 1% ^{10}B -loaded concrete.

Dose Estimates to the MIRD 5 Anthropomorphic Phantom

Different ^{10}B delivery agents can result in varying uptakes of boron in many of the body organs. These uptakes will vary with time after drug injection. In this section we calculate major organ doses during a patient irradiation assuming a uniform concentration of 10 ppm ^{10}B in all organs. Results are tabulated by dose component, including the ^{10}B dose from the reaction $^{10}\text{B}(n,\alpha)$. MCNP is used with the MIRD 5 anthropomorphic phantom model⁶. One can then scale these results for actual measured concentrations of ^{10}B in each organ. The quantifying of these doses is important and is the first step in deciding whether or not measures should be taken to reduce these doses.

Both BeO and Al/AlF₃ moderator designs are considered. A cutaway of the moderator/reflector design is shown in Fig. 5¹.

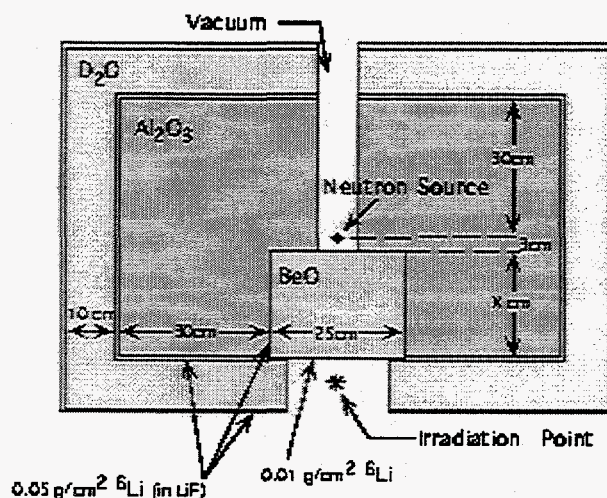


Figure 5: Design of moderator and reflector used for organ dose calculations. Both BeO and Al/AlF₃ moderators are investigated.

The moderator/reflector assembly together with the anthropomorphic phantom are shown in Fig. 6.

First, an estimate is made of the dose equivalent rate below the moderator/reflector assembly using the whole body dose conversion factors of Belogorlov⁴. This is done

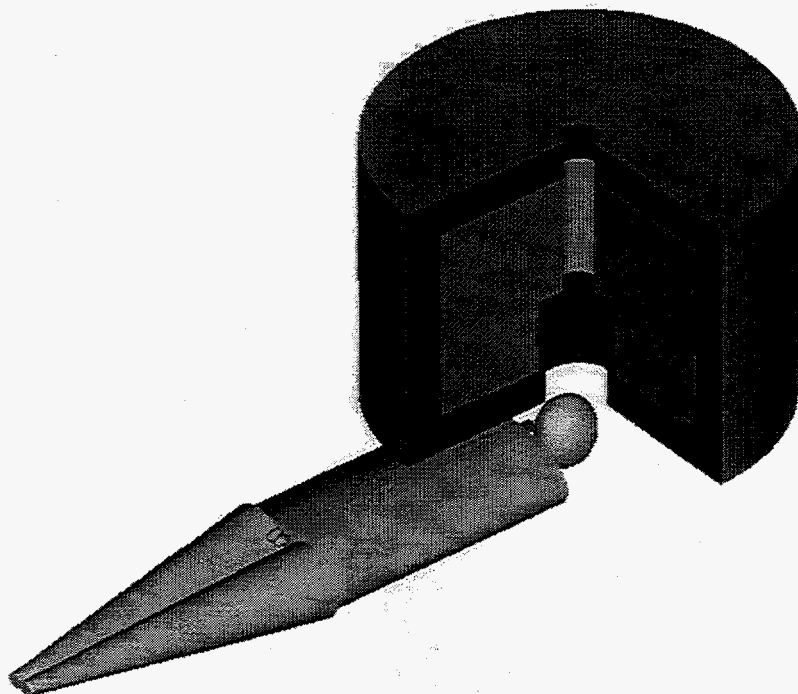


Figure 6: Layout of moderator/reflector assembly and anthropomorphic phantom used in MCNP calculations. Phantom internal organs not shown.

as a function of radial distance from the centerline of the moderator just below the irradiation point (See Fig. 5). MCNP point detectors are placed on a plane 1 cm below the bottom plane of the delimiter, from 0 to 60 cm radius. The resulting dose equivalent rates are shown in Fig. 7.

In order to calculate patient organ doses, the MIRD 5 anthropomorphic phantom⁶ is placed below the moderator/reflector assembly in the prone position as shown in Fig. 6. The anthropomorphic phantom used here is not the better known phantom of Christy and Eckerman⁷ but the differences are slight. The largest difference found in comparing the organ volumes was for the brain: 1470 cm³ for MIRD 5 and 1370 cm³ for Christy and Eckerman. These differences are not expected to be important for BNCT. The ICRU soft tissue adult male kerma factors⁸ are used for all organs. Boron kerma factors are taken from Caswell⁹. Three sets of kerma factors are used: one for soft tissue for both neutrons and photons and one

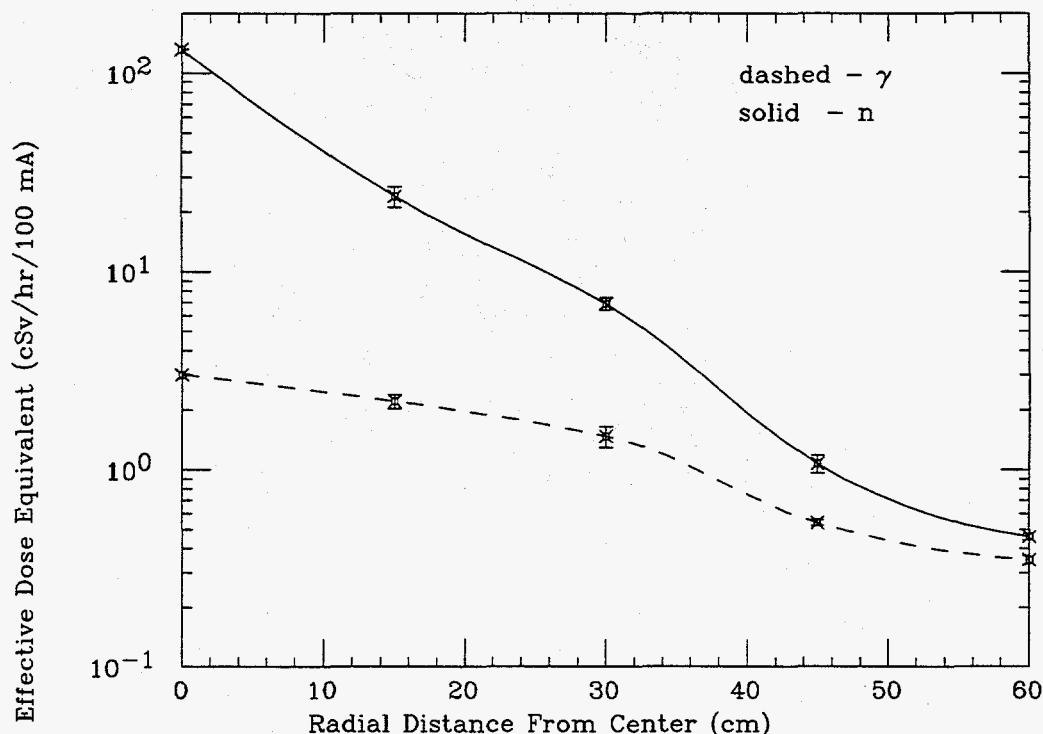


Figure 7: Variation of the effective dose equivalent from both neutrons and photons as a function of radial distance from the bottom center of the moderator/reflector assembly shown in Fig. 5. This calculation assumes the semi-infinite slab tissue equivalent fluence-to-dose conversion factors of Belogorlov⁴.

for ^{10}B . The complete neutron source energy spectrum used has been described previously¹. All doses and dose rates are normalized to a proton beam current of 20 mA. Elemental tissue and bone compositions used are shown in Table 4.

As a first step we benchmark the phantom results with our previous results¹⁰. In this work, the patient treatment planning software being developed at INEL, BNCT_rtp¹¹ (radiation treatment planning environment) was used to study the clinical efficacy of various moderators and proton beam energies. Patient head geometry was based on human MRI slices. Maximum tumor dose is scored at the point of maximum thermal neutron flux. In the phantom head considered in our work we have placed 10 spherical scoring volumes, representing tumors of 1 cm diameter, along the axis of the beam. These are placed at intervals of 1.5 cm center-to-center. The center of the first tumor scoring volume is located at a depth

Table 4: Elemental composition of the soft tissue bone and lung regions. Total densities of tissue, bone and lungs are 1.00, 1.4862 and 0.296 g/cm³, respectively.

Element	Weight Percent		
	Soft Tissue	Bone	Lungs
H	10.454	7.337	10.134
C	22.663	25.475	10.238
N	2.490	3.057	2.866
O	63.525	47.893	75.752
F	0.000	0.025	0.000
Na	0.112	0.326	0.184
Mg	0.013	0.112	0.007
Si	0.030	0.002	0.000
P	0.134	5.095	0.080
S	0.204	0.173	0.225
Cl	0.133	0.143	0.266
K	0.208	0.153	0.194
Ca	0.024	10.190	0.009
Fe	0.005	0.008	0.037
Zr	0.001	0.000	0.000

of 1.75 cm. Maximum tumor dose corresponds to that volume with the highest total dose. Results of the comparison are given in Table 5.

Table 5: Comparison of MCNP results for the anthropomorphic phantom with results from the INEL treatment planning code (see text) using a human CT scan.

Quantity	INEL-RTPE	MCNP/MIRD5	% difference
$\Phi_{th}(10^9 \text{ n}\cdot\text{cm}^{-2}\cdot\text{s}^{-1})$	1.77	1.66	6.2
$\dot{D}_B(\text{cGy}\cdot\text{RBE}\cdot\text{min}^{-1})^1$	13.1	11.2	14.7
$\dot{D}_n(\text{cGy}\cdot\text{RBE}\cdot\text{min}^{-1})^2$	6.8	8.22	20.9
$\dot{D}_\gamma(\text{cGy}\cdot\text{RBE}\cdot\text{min}^{-1})^3$	8.76	9.53	8.8
Time to 12.5 Gy (min)	43.6	43.6	—
D_T at max Φ_{th} (Gy-RBE)	65.3	57.5	11.2
D_T at 8 cm (Gy-RBE)	19.6	21.2	8.2

¹ RBE=1.3, 13 ppm ¹⁰B

² RBE=3.2, 13 ppm ¹⁰B, \dot{D}_n is the total neutron dose = fast + dose from ¹⁴N(n,p).

³ CF=3.8 (includes RBE) applied to \dot{D}_B , 45.5 ppm ¹⁰B

An uptake of 45.5 ppm ¹⁰B is assumed in tumor volumes and 13 ppm in normal tissues. An RBE of 3.2 is used for the neutron dose and a compound factor (including RBE) of 3.8 is used for the boron dose. These values are based on the BMRR Phase I clinical trials with BPA. The agreement between the MIRD 5

anthropomorphic phantom using MCNP and the INEL treatment software using human CT scans is quite good given the differences in calculational methods.

Table 6: Absorbed doses for different organs of the body, due to neutrons and gammas absorbed in soft tissue, and due to neutrons absorbed by ^{10}B for an arbitrary concentration of 10 mg of ^{10}B for 1 g of soft tissue (concentration = 10 ppm), moderator: BeO, Treatment time: 43.6 min. Relative errors in parentheses.

	Absorbed Dose Rate ($\text{cGy}\cdot\text{min}^{-1}\cdot 20\text{ mA}^{-1}$)						
	Brain	Adrenal	Lungs	Liver	Spleen	Kidneys	Testis
Neutron	5.80E-1 (0.01)	1.79E-3 (0.53)	5.42E-2 (0.03)	9.26E-3 (0.07)	3.09E-3 (0.23)	2.48E-4 (0.67)	5.59E-3 (0.40)
Gamma	5.33E0 (0.02)	5.79E-1 (0.25)	1.31E0 (0.03)	5.49E-1 (0.05)	4.26E-1 (0.12)	3.04E-1 (0.15)	1.54E-1 (0.40)
^{10}B	2.14E0 (0.01)	7.47E-3 (0.53)	2.24E-1 (0.03)	3.87E-2 (0.07)	1.29E-2 (0.23)	1.04E-3 (0.67)	2.33E-2 (0.40)
Total Rate ¹	9.97E0 (0.02)	5.94E-1 (0.26)	1.77E0 (0.03)	6.29E-1 (0.05)	4.53E-1 (0.14)	3.06E-1 (0.17)	2.02E-1 (0.40)
Total ²	4.35E2 (0.02)	2.59E1 (0.26)	7.74E1 (0.03)	2.74E1 (0.05)	1.97E1 (0.14)	1.33E1 (0.17)	8.81E0 (0.40)

¹ Total dose equivalent rate ($\text{cGy}\cdot\text{RBE}\cdot\text{min}^{-1}$ per 20 mA) over treatment time.

² Total dose equivalent ($\text{cGy}\cdot\text{RBE}$ per 20 mA) over treatment time.

Table 7: Same as Table 6 except moderator is Al/AlF₃ and treatment time is 39.7 minutes¹⁰.

	Absorbed Dose Rate ($\text{cGy}\cdot\text{min}^{-1}\cdot 20\text{ mA}^{-1}$)						
	Brain	Adrenal	Lungs	Liver	Spleen	Kidneys	Testis
Neutron	7.91E-1 (0.01)	1.78E-3 (1.00)	5.28E-2 (0.03)	8.09E-3 (0.07)	2.89E-3 (0.27)	1.61E-4 (0.85)	9.61E-3 (0.31)
Gamma	5.60E0 (0.01)	4.54E-1 (0.24)	1.19E0 (0.03)	4.91E-1 (0.05)	3.76E-1 (0.13)	2.52E-1 (0.15)	2.81E-1 (0.39)
^{10}B	2.54E0 (0.01)	7.38E-3 (1.00)	2.15E-1 (0.03)	3.34E-2 (0.07)	1.20E-2 (0.27)	7.00E-4 (0.85)	3.78E-2 (0.32)
Total Rate ¹	1.14E1 (0.01)	4.69E-1 (0.29)	1.64E0 (0.03)	5.60E-1 (0.04)	4.24E-1 (0.11)	2.53E-1 (0.14)	3.61E-1 (0.26)
Total ²	4.53E2 (0.01)	1.86E1 (0.29)	6.51E1 (0.03)	2.22E1 (0.04)	1.68E1 (0.11)	1.00E1 (0.14)	1.43E1 (0.26)

¹ Total dose equivalent rate ($\text{cGy}\cdot\text{RBE}\cdot\text{min}^{-1}$ per 20 mA) over treatment time.

² Total dose equivalent ($\text{cGy}\cdot\text{RBE}$ per 20 mA) over treatment time.

The estimated absorbed dose rates for select major organs are given in Table 6 for a BeO moderator and Table 7 for an Al/AlF₃ moderator. An arbitrary concentration

of 10 mg of ^{10}B for 1 g of soft tissue (concentration = 10 ppm) is assumed for all organs for scaling purposes. The ^{10}B dose component may be scaled accordingly for actual measured/estimated uptake in each organ to determine the actual organ dose. Of particular concern may be the boron uptake in blood-filtering organs such as the kidneys and liver. In general, for uniform boron uptake, those organs closest to the head receive the largest absorbed dose equivalents. The dose can be seen to drop about an order of magnitude from brain to lungs, and another order of magnitude from lungs to testes. Dose equivalents are lowest for the kidneys as they receive the most shielding effect from the body.

As stated previously, the kerma factors used for all organs were the ICRU soft tissue kermas from ICRU 46⁸. However, kerma factors for each specific organ are also available but were not used out of expediency. As a verification of this approximation, one case was run using the actual neutron kerma factors for the thyroid, lungs, liver and spleen. The ratio of the doses (real/approximation) were 0.89, 1.20, 1.0 and 1.0, respectively. These errors are roughly the same as the statistical errors given for the Monte Carlo simulations.

The ^{10}B dose equivalent contribution to the tumor from the moderator, as well as the dose equivalent contribution due to leakage from the reflector are shown in Fig. 8. The ratio of the reflector contribution to the moderator contribution is shown on the right axis. The reflector contribution was determined by making the bottom exit plane of the moderator a surface of zero importance in MCNP. In this way only particles leaking from the reflector, including those escaping the sides of the moderator into the reflector, are scored.

For shallow depths the ^{10}B dose equivalent represents about 90% of the total dose equivalent for both the moderator and the reflector contributions. For larger depths the ^{10}B dose equivalent represents an even greater percentage of the total dose equivalent. These results indicate that at a depth of about 8 to 9 cm, one-third of the tumor ^{10}B dose is a result of neutrons leaking from the surrounding reflector. This beneficial enhancement in ^{10}B dose for deep-seated tumors indicates

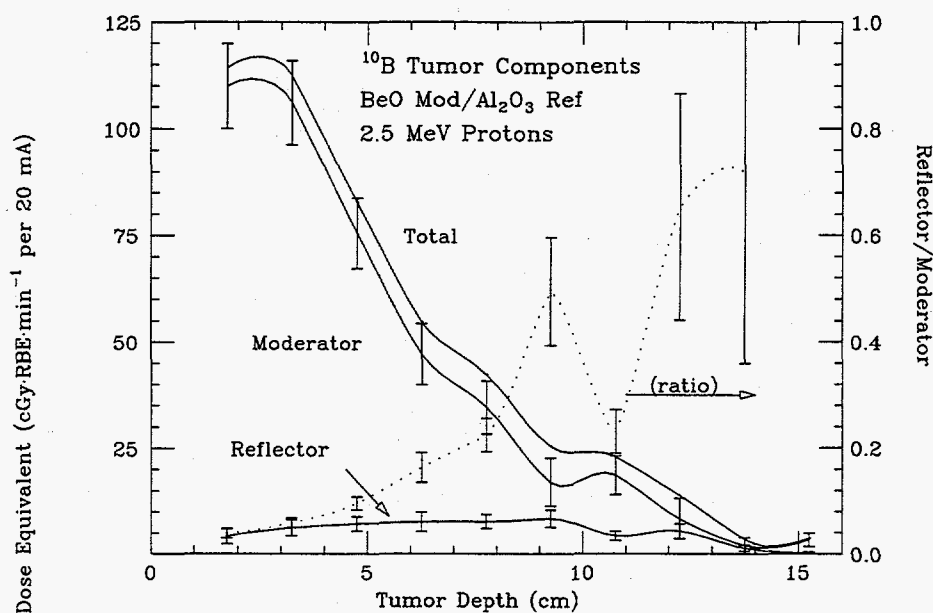


Figure 8: ^{10}B tumor dose contributions both directly from the moderator and leakage from the reflector, as a function of tumor depth in brain. ^{10}B concentration in tumor is 45.5 ppm.

Table 8: Percentage of normal tissue dose equivalent due to leakage from the reflector. Normal tissue ^{10}B concentration = 10 ppm. Results are for BeO moderator.

	Absorbed Dose Rate ($\text{cGy}\cdot\text{min}^{-1}\cdot 20\text{ mA}^{-1}$)						
	Brain	Adrenal	Lungs	Liver	Spleen	Kidneys	Testis
Neutron	15.8%	99.4%	95.4%	100%	100%	100%	100%
Gamma	23.2%	84.8%	91.6%	97.1%	94.8%	90.1%	100%
^{10}B	17.3%	99.6%	94.6%	99.2%	99.2%	97.1%	100%
Total Rate ¹	20.2%	85.2%	92.6%	97.3%	94.9%	90.2%	100%

¹ Total dose equivalent rate ($\text{cGy}\cdot\text{RBE}\cdot\text{min}^{-1}$ per 20 mA) over treatment time.

that additional optimization work should investigate the role of leakage radiation in tumor and normal tissue brain dose.

Acknowledgements

We wish to thank Mark Konijnenberg of the Mallinckrodt Medical BV (Petten, The Netherlands) who shared his input for the geometry of the MIRD 5 anthropomorphic phantom used in our simulation.

We thank Darren Bleuel (UC Berkeley) for many useful discussions.

References

1. D. L. Bleuel and R. J. Donahue, "Optimization of the ${}^7\text{Li}(p,n)$ Proton Beam Energy for BNCT Applications" LBL-37983 Revision 1, May (1996).
2. W. S. Snyder, M. R. Ford and G. G. Ford, "Estimates of Specific Absorbed Fractions for Photon Sources Uniformly Distributed in Various Organs of a Heterogeneous Phantom", MIRD Pamphlet No. 5 Revised, Society of Nuclear Medicine, New York (1978).
3. "MCNP-A A General Monte Carlo N-Particle Transport Code, Version 4A," J. F. Briesmeister, Ed. , LA-12625, Los Alamos National Lab. (1993).
4. Belogorlov, *et al.*, *Depth Dose and Depth Dose Equivalent Data for Neutrons with Energy from Thermal up to Several TeV*, NIM **199** (1982) 563-572.
5. A. B. Chilton *et al.*, Principles of Radiation Shielding, Prentice-Hall (1984).
6. M. Christy, "Mathematical Phantoms Representing Children of Various Ages for Use in Estimates of Internal Dose", NUREG/CR-1159, Oak Ridge National Laboratory, March (1982).
7. M. Christy and K. F. Eckerman, "Specific Absorbed Fractions of Energy at Various Ages from Internal Photon Sources", Oak Ridge National Laboratory, ORNL/NUREG/TM-8381: Volume 1 (1987).
8. "Photon, Electron, Proton and Neutron Interaction Data for Body Tissues", ICRU Report 46, February (1992).

9. R. S. Caswell, J. J. Coyne and M. L. Randolph, "Kerma Factors for Neutron Energies Below 30 MeV", *Radiation Research* **83** 217 (1980).
10. D. L. Bleuel, R. J. Donahue and B. A. Ludewigt, "On Optimizing the ${}^7\text{Li}(p,n)$ Proton Beam Energy and Moderator Material for BNCT", to be published in the Proceedings of the 14th International Conference on the Application of Accelerators in Research and Industry, Denton Texas, November 6-9 (1996).
11. D. W. Nigg *et al.*, "Methods for Radiation Dose Distribution Analysis and Treatment Planning in Boron Neutron Capture Therapy", *Int. Journal of Rad. Oncology Bio:Phys*, **28** 1121-1134 (1994).